Electronic Supplementary Material (ESI) for Soft Matter.

Supporting Information

Smart Design of Wettability-Patterned Gradient on Substrate-Independent Coated Surfaces to Control Unidirectional Spreading of Droplet

Huaping Wu,*[a,c] Kai Zhu,[a] Binbin Cao,[a] Zheng Zhang,[a] Bingbing Wu,[a] Lihua Liang,[a] Guozhong Chai[a] and Aiping Liu*[b]

[a] *Key Laboratory of E&M (Zhejiang University of Technology), Ministry of Education & Zhejiang Province, Hangzhou 310014, China.*

[b] *Center for Optoelectronics Materials and Devices, Zhejiang Sci-Tech University, Hangzhou 310018, China.*

[c] *State Key Laboratory of Structural Analysis for Industrial Equipment, Dalian University of Technology, Dalian 116024, China*

Table of context:

Supplementary Analysis I:

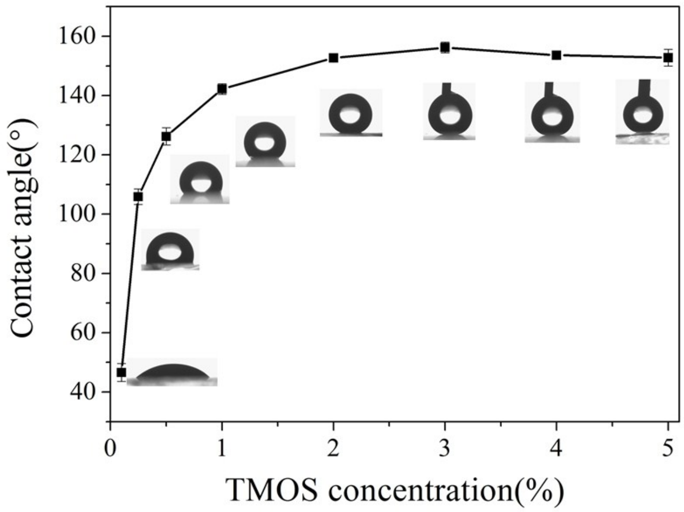

Figure S1. Effect of TMOS concentration on water contact angle on glass substrate.

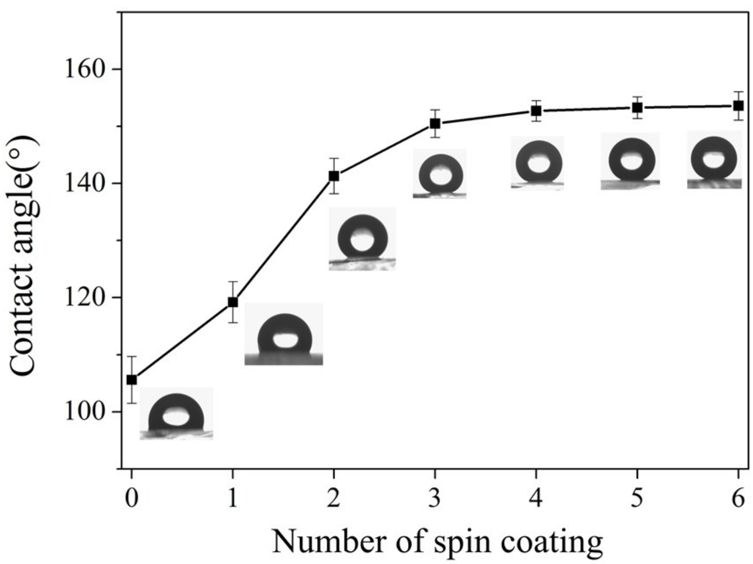

Figure S2. Effect of the number of spin coating on water contact angle on glass substrate.

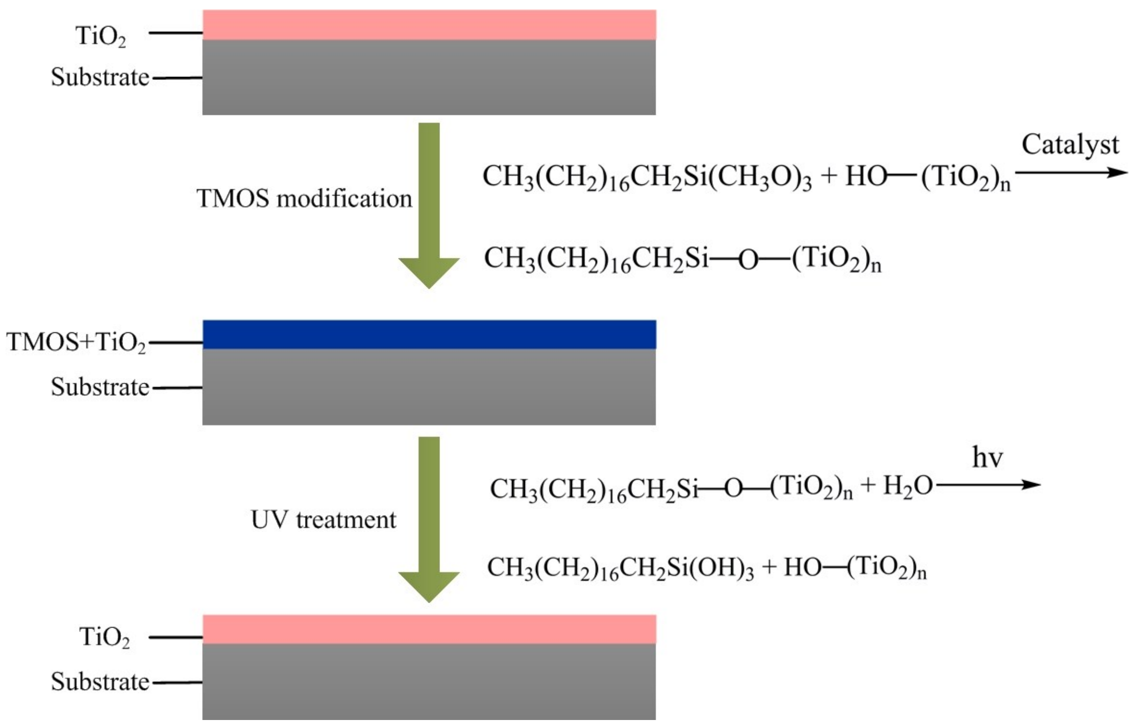

Figure S3. Reaction mechanism during the modification of TiO_2 with TMOS before and after UV irradiation.

Table S1. XPS analysis of TMOS-TiO_2 coatings before and after UV irradiation for 30 minutes.

Sample	**Atomic concentration (at.%)**			
	O	**Ti**	**C**	**Si**
TMOS-TiO_2	33.8	11.0	49.3	5.9
UV irradiated TMOS-TiO_2	61.8	19.9	11.1	7.2

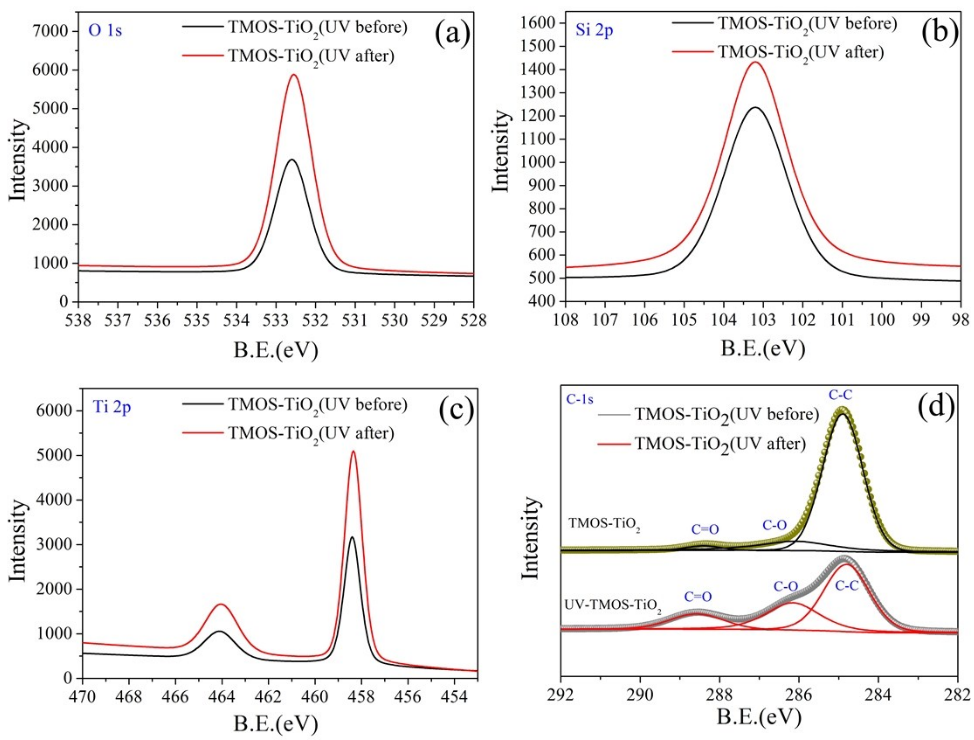

Figure S4. XPS spectra of (a) O 1s, (b) Si 2p ,(c) Ti 2p and (d) C 1s for the TMOS-TiO_2 coatings before and after UV irradiation for 30 minutes.

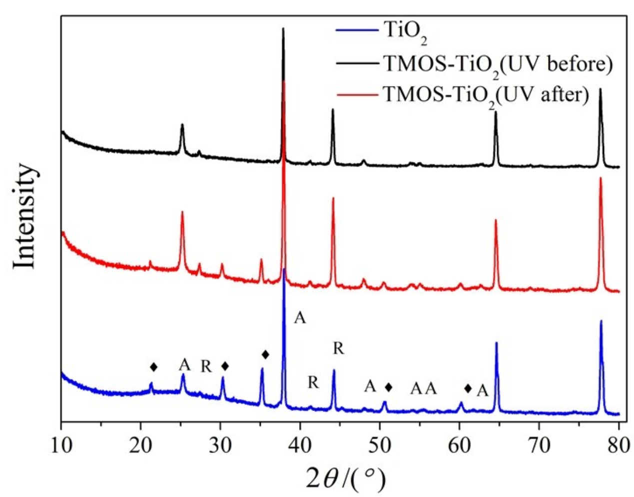

Figure S5. XRD patterns of TiO_2 and TMOS-TiO_2 coatings before and after UV irradiation for 30 minutes. (A: anatase; R: rutile).

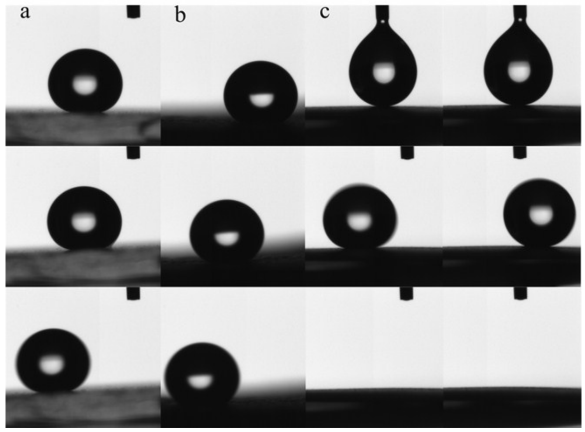

Figure S6. Sliding angles of a droplet on the TMOS-TiO_2 coated (a) glass sheet (3.0°) and (b) dustlessness cloth (2.9°). (c) The adhesion of a droplet on the TMOS-TiO_2 coated filter paper was lower than on the glass sheet and dustlessness cloth. The droplet could be hardly deposited on a specific area of the filter paper and easily roll away due to weak adhesion. The water droplets were 10 μL in volume.

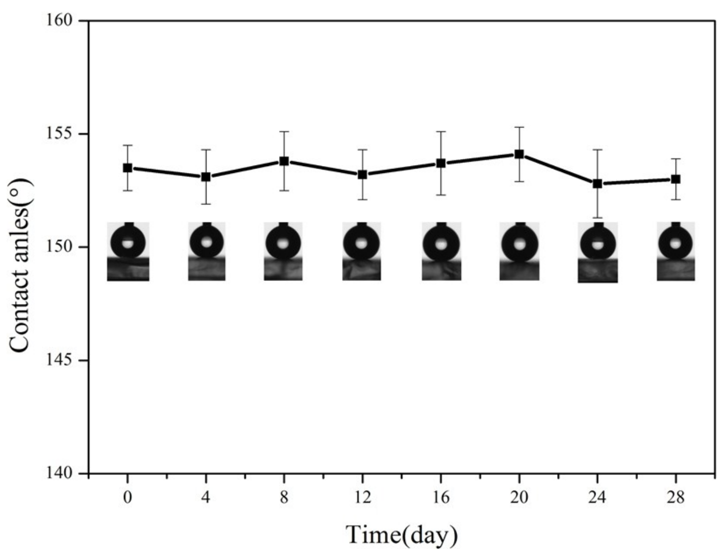

Figure S7. Long-term stability of TMOS-TiO_2 coated glass sheet. The test of the water contact angles was carried out under ambient atmospheric condition every four days for a month.

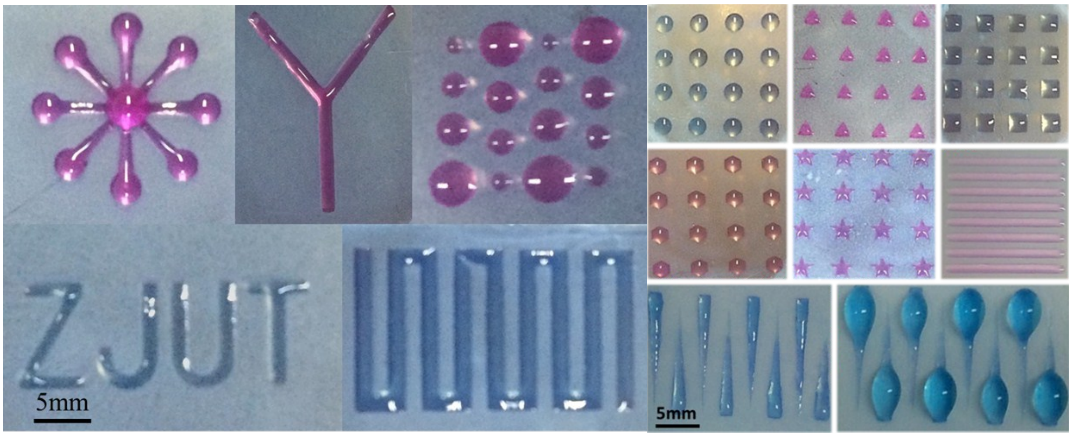

Figure S8. Superhydrophilic patterns with different geometries and sizes filled with dye solutions on TMOS–TiO_2 coated substrates.

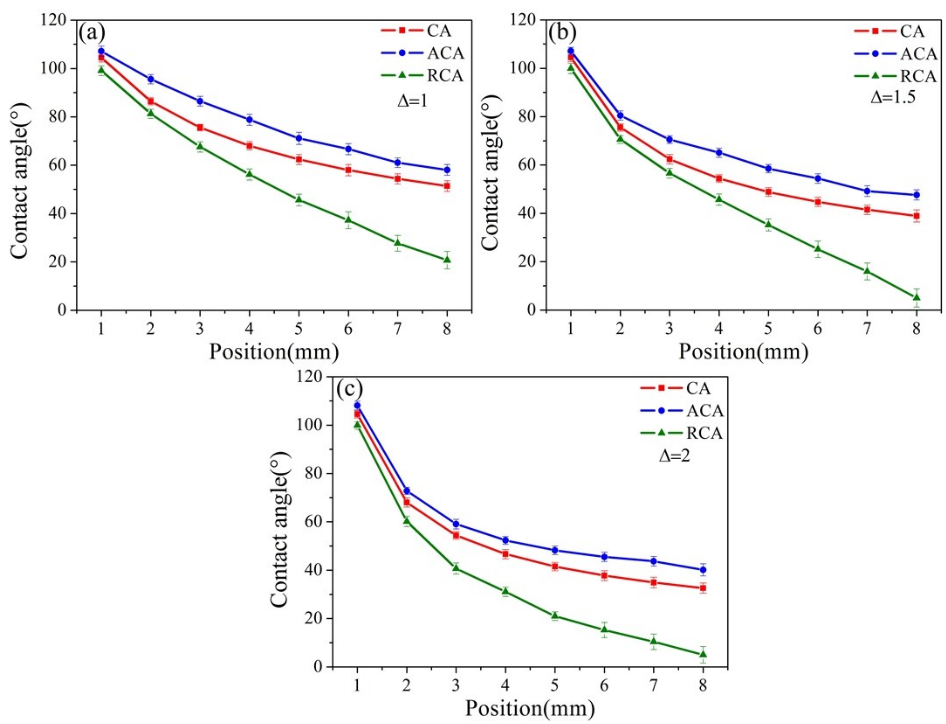

Figure S9. Water contact angles (CAs), advancing contact angles (ACAs) and receding contact angles (RCAs) as functions of positions on three unidirectional channels with the spacing *P* between two adjacent stripes of (a) 20 μm, (b) 30 μm and (c) 40 μm.

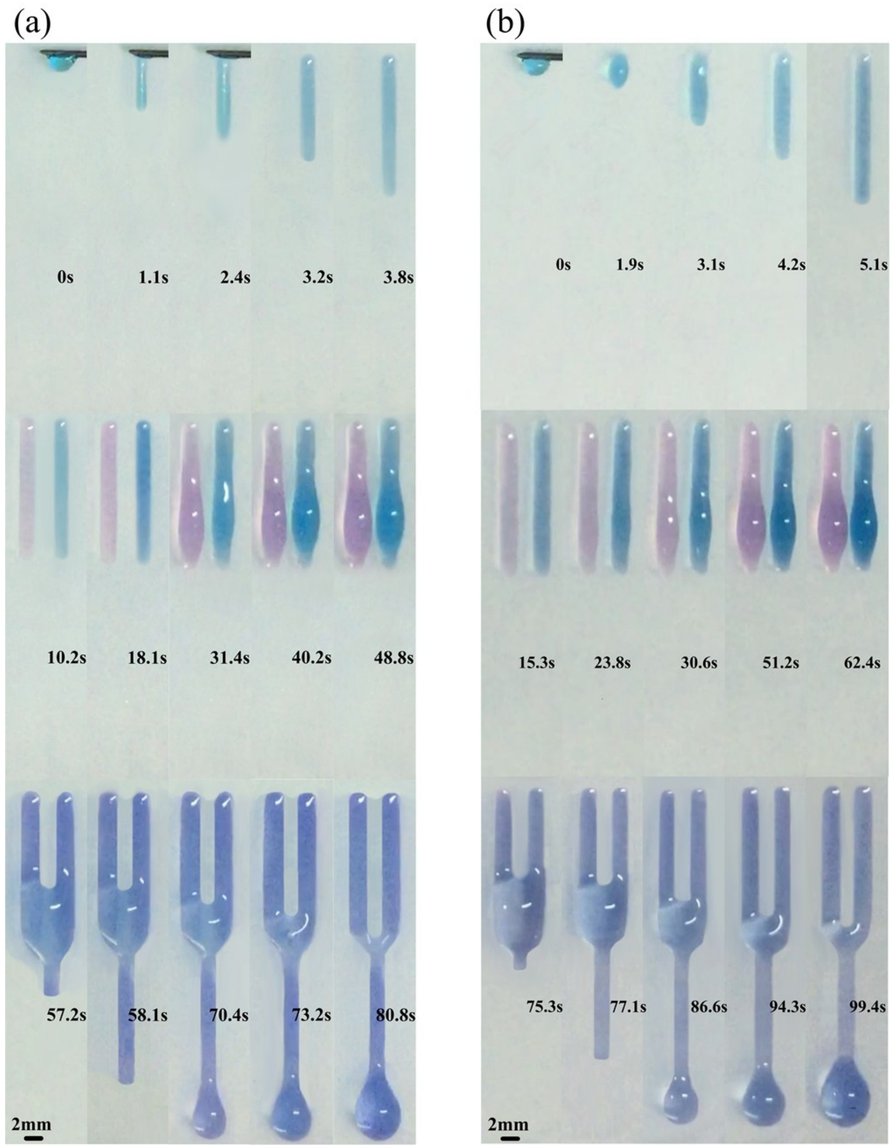

Figure S10. Time-lapsed images of different concentrated liquid transport, bridging and draining: (a) V_{water}: $V_{ethanol}$=2:1; (b) V_{water}: $V_{ethanol}$=4:1. The scale bar is 2 mm.

Supplementary Analysis II:

Droplet motion on wettability-patterned gradient surface

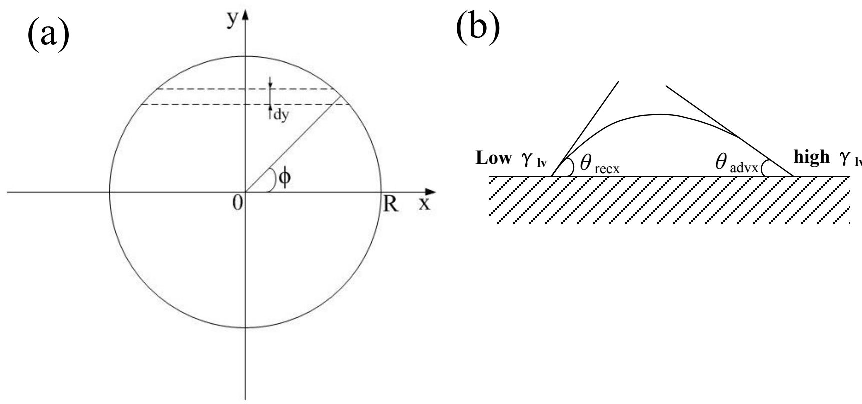

Figure S11. Schematic illustration of drop motion

As can be seen from Figure S11, for a thin strip of liquid thickness *dy* parallel to the spreading direction, the wettability gradient force (F_D) at the *k* location which drives the droplet toward more wettable region of the surface can be described as[33,37,38,78]

$$\begin{aligned} F_D &= \gamma_{lv}\int_{-R}^{R}\left[(\gamma_{SV}-\gamma_{SL})_n-(\gamma_{SV}-\gamma_{SL})_0\right]dy \\ &=2R\int_0^{\frac{\pi}{2}}\left[(\gamma_{SV}-\gamma_{SL})_n-(\gamma_{SV}-\gamma_{SL})_0\right]\cos\phi d\phi \end{aligned} \quad . \qquad \text{S(1)}$$

According to the Young's equation, $\gamma_{LV}=\frac{\gamma_{SV}-\gamma_{SL}}{\cos\theta}$, the F_D can be rewritten as

$$\begin{aligned} F_D &= 2R\int_0^{\frac{\pi}{2}}\gamma_{LV}(\cos\theta_n-\cos\theta_0)\cos\phi d\phi \\ &= 2R\int_0^{\frac{\pi}{2}}\gamma_{LV}(\cos\theta_n-\cos\theta_{n-1}+\cos\theta_{n-1}-\cos\theta_{n-2}+...+\cos\theta_1-\cos\theta_0)\cos\phi d\phi \\ &= 2R\gamma_{LV}\sum_{n=1}^{k}\left(\cos\theta_n-\cos\theta_{n-1}\right) \end{aligned} \quad , \qquad \text{S(2)}$$

where *R* is the base radius of the droplet to contact surface in the *x* direction just before unidirectional spread, and γ_{LV} is the surface tension of droplet. θ_n corresponds to the apparent contact angle of droplet on the n^th wettability pattern of one channel. The similar technique based on Eq. (2) can be applied for the analysis of hysteresis force (F_H)

$$F_H = 2R\gamma_{lv}\sum_{n=1}^{k}\int_0^{\frac{\pi}{2}}(\cos\theta_{rn} - \cos\theta_{an})\cos\phi d\phi = 2R\gamma_{lv}\sum_{n=1}^{k}\left(\cos\theta_{rn} - \cos\theta_{an}\right) \quad , \qquad S(3)$$

where θ_{an} and θ_{rn} correspond to the advancing contact angle and the receding contact angle on the n^th wettability pattern of one channel.